

CMUA-Watermark: A Cross-Model Universal Adversarial Watermark for Combating Deepfakes

Hao Huang¹, Yongtao Wang¹, Zhaoyu Chen², Yuheng Li¹, Zhi Tang¹, Wei Chu³, Jingdong Chen³,
Weisi Lin⁴, Kai-Kuang Ma⁴

¹ Peking University, Beijing, China

² Fudan University, Shanghai, China

³ Ant Group, Beijing, China

⁴ Nanyang Technological University, Singapore

huanghao@stu.pku.edu.cn, {wyt, tangzhi}@pku.edu.cn, zhaoyuchen20@fudan.edu.cn, yuhengli2021@outlook.com,
{weichu.cw, jingdongchen.cjd}@antgroup.com, {wslin, ekkma}@ntu.edu.sg

Abstract—Malicious application of deepfakes (i.e., technologies can generate target faces or face attributes) has posed a huge threat to our society. The fake multimedia content generated by deepfake models can harm the reputation and even threaten the property of the person who has been impersonated. Fortunately, the adversarial watermark could be used for combating deepfake models, leading them to generate distorted images. The existing methods require an individual training process for every facial image, to generate the adversarial watermark against a specific deepfake model, which are extremely inefficient. To address this problem, we propose a universal adversarial attack method on deepfake models, to generate a Cross-Model Universal Adversarial Watermark (CMUA-Watermark) that can protect thousands of facial images from multiple deepfake models. Specifically, we first propose a cross-model universal attack pipeline by attacking multiple deepfake models and combining gradients from these models iteratively. Then we introduce a batch-based method to alleviate the conflict of adversarial watermarks generated by different facial images. Finally, we design a more reasonable and comprehensive evaluation method for evaluating the effectiveness of the adversarial watermark. Experimental results demonstrate that the proposed CMUA-Watermark can effectively distort the fake facial images generated by deepfake models and successfully protect facial images from deepfakes in real scenes.

1. Introduction

Recently, the great improvement of Generative Adversarial Networks (GANs) has shown the impressive results for virtual content generation. However, virtual content generated by GANs also poses a great threat to our society (e.g., Deepfake Image/Video). Deepfake (a portmanteau of "deep learning" and "fake"), referring to a deep learning based face modification networks to generate fake content of target person or target attributes by GANs, has caused great harm to some people, especially public figures. On the one hand, fake images and videos can show things that a person has

never said or done, which might cause damage to his/her reputation, especially when it comes to pornography or politics. On the other hand, fake faces with target attributes may pass the verification of commercial applications, threatening the application security and harming the property of the person who has been impersonated.

Generally speaking, there are two ways to mitigate the risk of deepfakes. One is training deepfake detectors [4], [5], [6], [7], [8], [9], [10] to detect the modified content, and the other is attacking the deepfake model to generate an adversarial perturbation [11]. Such a perturbation can be treated as an **Adversarial Watermark** to combat deepfake models, leading the models to generate obviously unreal outputs. However, the method proposed in [11] could only generate an adversarial watermark for a specific image against a specific deepfake model by an individual training process. Obviously, it is extremely time-consuming and unworthy to generate such watermarks with low generalization for thousands of facial images.

To address these issues, we propose an effective and efficient universal attack method, which can generate the adversarial watermark for protecting thousands of facial images from multiple deepfake models. According to the generalization ability of the universal adversarial watermarks, we divide them into the following categories:

- 1) SIA-Watermark: A single-image adversarial watermark that can protect a single image from one deepfake model. The watermark in [11] falls into this category.
- 2) CIUA-Watermark: A cross-image universal adversarial watermark that can protect multiple images from one deepfake model.
- 3) CMUA-watermark: A cross-model universal adversarial watermark that can protect multiple images from multiple deepfake models. Our CMUA-watermark falls into this category.

In a sense, generating a CIUA-Watermark is to find the intersection of data weaknesses, while generating a CMUA-watermark is to find the intersection of data weaknesses and

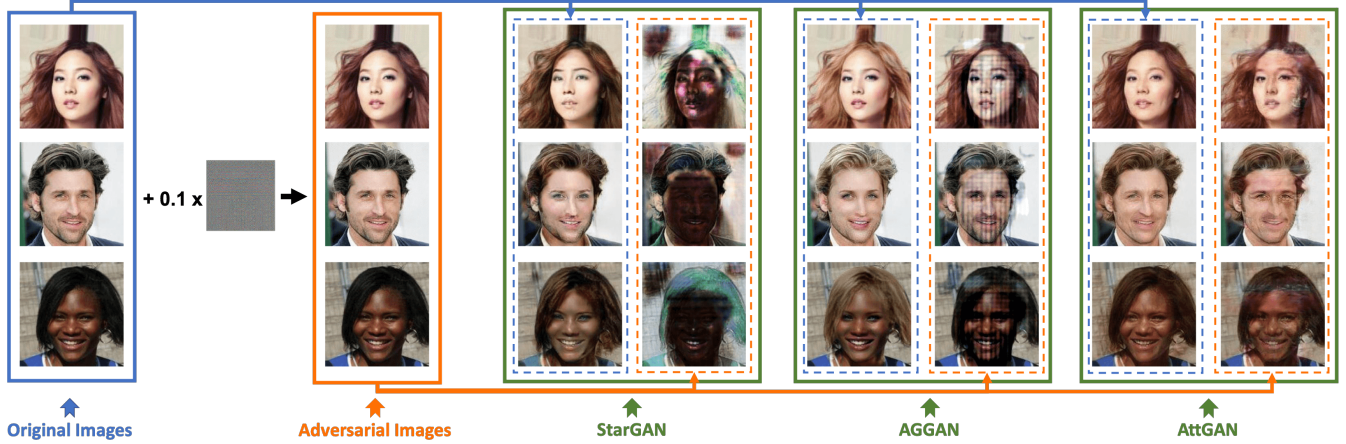


Figure 1. Illustration of our CMUA-Watermark. Once the CMUA-watermark has been generated from training, we can directly add it to any facial image to generate an adversarial facial image which is visually same as the original image but can make deepfake models like StarGAN [1], AGGAN [2] and AttGAN [3] output distorted image. In this way, we can protect facial images from deepfake models.

model weaknesses simultaneously. To achieve this goal, we propose a cross-model universal attack pipeline for deepfake models. Firstly, we input a batch of facial images into multiple deepfake models to get the adversarial watermarks per image. However, due to the unique attributes of the specific facial image, these watermarks may conflict with each other. Then, to alleviate the conflict and enhance the performance of universal adversarial watermark, we average a large batch of watermarks generated by facial images to get an averaged watermark, which can lead the watermark to focus on common attributes of human faces rather than the unique attributes of one specific image. Next, we iteratively attack multiple deepfake models to refine our adversarial watermark step by step. Finally, the well-trained CMUA-watermark can be added into human facial images to protect them from multiple deepfake models.

To judge whether an image is successfully protected is not easy, and the existing evaluation method in [11] is not comprehensive enough since it only focuses on L_1/L_2 distance between the fake images generated by **adversarial examples** ($FakeFace_a$) and the fake images generated by **clean images** ($FakeFace_c$). According to our original purposes, we design a more reasonable and comprehensive evaluation method. On the one hand, we require that the adversarial watermark needs to lower the quality of the $FakeFace_a$ and maximize the difference between $FakeFace_a$ and the $FakeFace_c$. Specifically, we use Fréchet Inception Distance (FID) [12] to measure the quality of the generated fake faces, use L_2 distance to measure the distortion between the $FakeFace_a$ and the $FakeFace_c$, and use PSNR, SSIM [13] and LPIPS [14] to measure the similarity between the $FakeFace_a$ and the $FakeFace_c$. On the other hand, we require that the adversarial watermark needs to make the fake faces unable to pass the liveness detection system, which commercial applications use to ensure the image is from a true person.

Therefore, we regard the confidence score and passing rate of the liveness detection system as another two metrics.

Experimental results demonstrate that our CMUA-Watermark can effectively protect facial images from multiple deepfake models (as illustrated in Figure 1) and can successfully prevent the fake facial images passing the verification of liveness detection system of commercial applications.

Our contributions can be summarized as:

- We first introduce a novel idea of generating cross-model universal adversarial watermark (CMUA-Watermark) to protect human facial images from deepfakes.
- We propose a cross-model universal attack pipeline to generate CMUA-Watermark against multiple deepfake models by iteratively averaging the adversarial watermarks which are generated from multiple facial images.
- We design a more reasonable and comprehensive evaluation method to fully evaluate the effectiveness of the adversarial watermark for combating deepfakes.
- We achieve very effective performance for protecting facial images from deepfakes, even in real scenes.

2. Related Works

2.1. Face Modification

In recent years, the free access to large-scale facial images and the amazing progress of generative models have led face modification networks to generate more real fake facial images with target person or attributes.

StarGAN [1] proposes a novel and scalable approach to perform image-to-image translation across multiple domains. Compared to previous methods [15], [16], [17], the

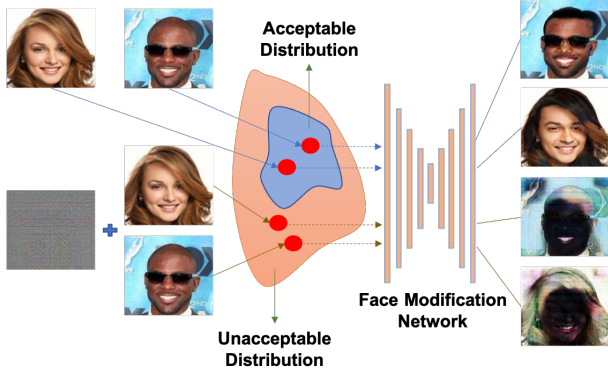


Figure 2. Illustration of CIUA-Watermark. Essentially, the CIUA-Watermark is a well-designed perturbation which tries to make the facial image is out of the acceptable distribution of the specific model.

generated images by StarGAN have achieved better visual quality. To address the problem that the strict attribute-independent constraint on the latent representation leads to over-smooth and distorted generation, AttGAN [3] removes it and just uses the attribute-classification constraint to provide more real fake images on facial attribute manipulation. Moreover, AGGAN [2] introduces the attention masks via a built-in attention mechanism to obtain target images with high quality.

Though these methods adopt diverse architectures and losses, our CMUA-watermark can prevent the facial images being modified correctly by them.

2.2. Attacks on Generative Model

There are already some studies [11], [18], [19], [20], [21], [22] that explore the adversarial attacks on the generative models (i.e., GANs) and we focus on the attacks on image translation. [18] and [19] adapt adversarial attacks to image translation on CycleGAN [17] and pix2pixHD [23] which only transfer images between two domains so they are relatively easy to attack. [11] first addresses disruptions on conditional image translation networks but the watermark they generated is SIA-Watermark. In other words, such a perturbation with low generalization can only protect a specific image from a specific deepfake model.

Compared to [11], the proposed cross-model universal attack method generates CMUA-watermark with high generalization, which can protect thousands of facial images from multiple deepfake models without individual training for every image.

2.3. Universal Adversarial Watermark

Universal Adversarial Perturbation is first introduced by [24] that can fool a recognition model with only a single adversarial perturbation. Here the *Universal* means the single perturbation can be added to multiple images to fool one model. [25] introduces universal adversarial perturbation for the segmentation task to generate target results. [26] first

proposes a universal adversarial attack against the image retrieval system which can lead the system to return irrelevant images.

Compared to the works [24], [25], [26], [27], [28] which can only produce universal adversarial watermark for one model, we propose a cross-model universal attack method on face modification networks, that is, our universal adversarial perturbation can combat multiple face modification models simultaneously.

3. Method

In this section, we introduce our method in detail. Firstly, we introduce how to attack an image translation network in Section 3.1. Then, we describe the cross-image and cross-model universal adversarial attack in Section 3.2 and 3.3 respectively.

3.1. Attacks on Face Modification Model

In our work, we propose a universal adversarial attack method to attack multiple face modification models, and generate an adversarial watermark w . Our goals are to lower the quality of the $FakeFace_a$, maximize the difference between the $FakeFace_a$ and $FakeFace_c$, and make the $FakeFace_a$ fail to pass the verification of the liveness detection system. We use Mean Squared Error (MSE) to measure the difference between the $FakeFace_a$ and $FakeFace_c$, that is,

$$\max_w MSE(FakeFace_a, FakeFace_c). \quad (1)$$

Moreover, the adversarial watermark w should be imperceptible to human eyes to ensure the visual quality of protected facial images. Hence, we introduce a constraint that:

$$\|w\|_\infty \leq \epsilon, \quad (2)$$

where ϵ is the upper bound magnitude of the watermark.

3.2. Cross-Image Universal Adversarial Attack

In this section, we describe how to train a CIUA-Watermark to protect multiple facial images from one face modification network. Generally speaking, every well-trained face modification network has its own acceptable input data distribution which means that only the facial images that satisfy the acceptable distribution of the network can be modified correctly. Due to the large-scale training data, almost all of the natural facial images satisfy this acceptable distribution. However, the adversarial perturbation can lead the natural facial images to out of the acceptable distribution. So, the CIUA-Watermark is such a perturbation that tries to lead all the natural facial images to out of the acceptable distribution of a specific model as Figure 2 shows.

We use I-FGSM [29] to generate perturbations at every attack iteration. These perturbations are further combined to form a universal perturbation by a decay factor m :

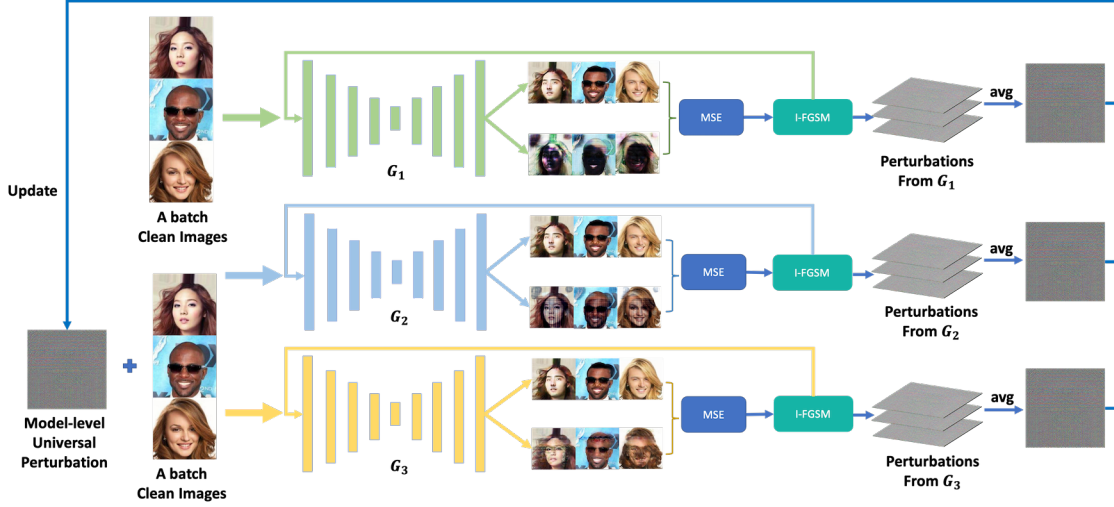


Figure 3. The whole pipeline of our cross-model universal adversarial attack on multiple face modification networks.

TABLE 1. THE QUANTITATIVE RESULTS OF CIUA-WATERMARK ON CELEBA TEST SET

Source Model->Target Model	L2↑	Success Rate [11]↑	PSNR↓	SSIM↓	LPIPS↑	FID↑	ACS↓	TFHC↓	TFLC↓
StarGAN->StarGAN	1.048	100%	6.087	-0.027	0.591	239.422	0.914->0.002	66.26%->0%	80.42%->0%
StarGAN->AGGAN	0.054	42.13%	19.362	0.634	0.149	5.524	0.928->0.900	65.88%->65.87%	81.46%->72.23%
StarGAN->AttGAN	0.000	0%	44.490	0.978	0.004	3.814	0.872->0.871	55.13%->55.07%	71.20%->71.08%
AGGAN->StarGAN	0.202	100%	13.230	0.358	0.378	67.612	0.914->0.618	66.26%->13.25%	80.42%->28.94%
AGGAN->AGGAN	0.368	100%	11.120	0.480	0.280	31.502	0.928->0.875	65.88%->39.82%	81.46%->64.35%
AGGAN->AttGAN	0.000	0%	41.233	0.964	0.008	3.877	0.872->0.868	55.13%->54.22%	81.46%->70.42%
AttGAN->StarGAN	0.027	8.55%	22.318	0.577	0.202	46.135	0.914->0.899	66.26%->67.80%	80.42%->80.96%
AttGAN->AGGAN	0.037	25.51%	21.643	0.622	0.211	40.389	0.928->0.834	65.88%->50.22%	81.46%->67.46%
AttGAN->AttGAN	0.062	49.51%	18.956	0.507	0.328	60.339	0.872->0.770	55.13%->45.45%	81.46%->62.55%

TABLE 2. THE QUANTITATIVE RESULTS OF CMUA-WATERMARK WITH DIFFERENT DATASETS

Dataset	Model	L2↑	Success Rate [11]↑	PSNR↓	SSIM↓	LPIPS↑	FID↑	ACS↓	TFHC↓	TFLC↓
CelebA	StarGAN	0.457	100%	9.651	0.121	0.459	115.312	0.914->0.345	66.26%->9.26%	80.42%->19.78%
	AGGAN	0.107	99.21%	16.227	0.476	0.298	87.169	0.928->0.670	65.88%->22.30%	81.46%->43.72%
	AttGAN	0.037	20.20%	21.894	0.599	0.242	38.472	0.872->0.738	55.13%->38.35%	71.20%->55.50%
LFW	StarGAN	0.433	100%	9.814	0.124	0.513	114.441	0.737->0.161	43.88%->3.01%	58.94%->7.20%
	AGGAN	0.101	99.66%	16.527	0.503	0.261	45.701	0.863->0.627	54.91%->18.16%	72.31%->37.47%
	AttGAN	0.041	22.75%	21.432	0.569	0.261	45.593	0.586->0.507	25.87%->19.00%	40.08%->32.41%

$$P_{batch}^{avg} = \frac{\sum_j^{bs} A_{base}(x_j, L, G, a)}{bs}, \quad (3)$$

$$w_i = clip(w_{i-1} * m + P_{batch}^{avg} * (1 - m), -\epsilon, \epsilon),$$

where bs is the batch size of facial images, A_{base} is the base attack algorithm (e.g., I-FGSM [29] or PGD [30]) which returns the adversarial perturbation P of the clean facial image x_j , L is the loss function (we exploit MSE as formulated in Eq.(1)), G is the face modification network we attack, a is the step size in base attack, w_i is the training universal perturbation at i th iteration, $m \in (0, 1)$ is a parameter to control the update ratio at every iteration, ϵ is the upper bound magnitude of the training watermark, and the operation $clip$ limits the magnitude of w_i in the range of $[-\epsilon, \epsilon]$.

Training a universal perturbation is not easy because the perturbations in every iteration generated by different facial images may conflict with each other. To address the issue, we propose a batch-based universal attack method. In every iteration, we input bs facial images to calculate bs perturbations. Then, for alleviating the conflict of these perturbations and making the universal watermark focus on the common attributes of human faces, we get an averaged perturbation by taking the average of these perturbations to update the training universal perturbation.

3.3. Cross-Model Universal Adversarial Attack

The cross-model universal adversarial attack is based on the cross-image attack, and needs to further find the intersection of unacceptable distribution from multiple models.

The whole pipeline we train CMUA-Watermark is shown in Figure 3.

Firstly, we input a batch of clean facial images and a batch of clean facial images with the initial universal perturbation to multiple face modification models. The value of initial universal perturbation depends on which base attack method we select (e.g., all-zero for I-FGSM and random noise for PGD). Then, for each model, we calculate the MSE loss of their outputs and use I-FGSM to get the perturbation of each image. After that, we average the perturbations of each model at every iteration (every batch). Finally, we use Eq.(3) to update the CMUA-Watermark, and we update n times per iteration to attack n models. After sufficient training, we can get an effective CMUA-Watermark to protect any facial image. The details of our cross-model attack can be referred to Algorithm 1.

Algorithm 1 cross-model universal attack on multiple face modification networks

Input: G_k (the k th face modification network we combat), k_{max} (the number of face modification networks we need to combat), X_j (the training images of j th batch), j_{max} (the maximum number of training batch), L (loss function), w_j (universal adversarial watermark in j th iteration), A_{max} (the maximum number of attack iteration per batch), a (the step size in attack).

Output: CMUA-Watermark W

```

1: Init.  $w_0$ 
2: for each  $j \in [1, j_{max}]$  do
3:    $\tilde{X}_j \leftarrow X_j + w_{j-1}$ 
4:   for each  $k \in [1, k_{max}]$  do
5:      $P_{batch} \leftarrow 0$ 
6:     for each  $iter \in [1, A_{max}]$  do
7:        $P_{batch} \leftarrow a * \text{sign} [\nabla_{X_j} L(G(X_j), G(\tilde{X}_j))]$ 
8:        $\tilde{X}_j \leftarrow \text{clip}(\tilde{X}_j + P_{batch})$ 
9:     end for
10:     $P_{batch}^{avg} \leftarrow \text{avg}(P_{batch})$ 
11:    use  $P_{batch}^{avg}$  to update  $w_j$  on  $G_k$  according to Eq.(3)
12:  end for
13: end for
14: return  $w_j$ 

```

4. Experiment

In this section, we first describe our datasets and implementation details in Section 4.1. Then, we introduce our evaluation metrics in Section 4.2. After that, we show the experimental results of CIUA-Watermark and CMUA-Watermark in Section 4.3 and Section 4.4 respectively. Furthermore, we systemically investigate the influence of hyperparameters on the watermark in Section 4.5. Finally, in Section 4.6, we test the effectiveness of CMUA-Watermark in more real scenes.

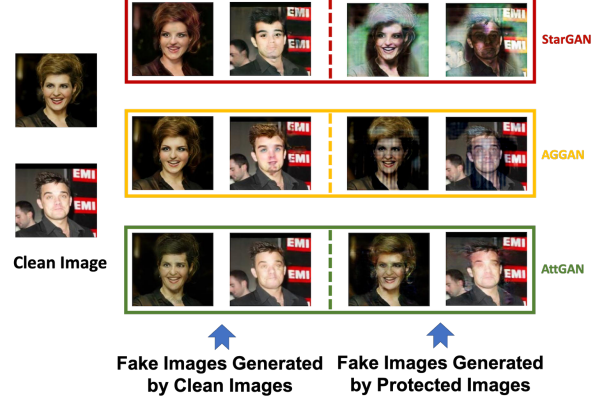


Figure 4. Illustration of two examples on LFW.

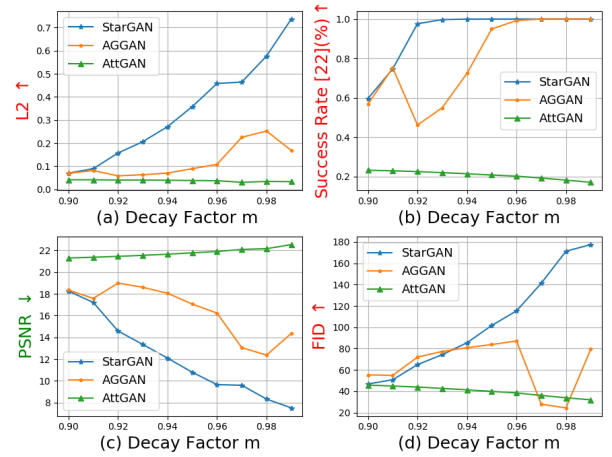


Figure 5. The curves of L_2 , Success Rate [11], PSNR and FID with the decay factor m .

4.1. Datasets and Implementation Details

In our experiments, we use CelebA [31] test set as the main dataset which contains 19962 facial images. To further evaluate the generalization ability of our CMUA-Watermark, we also generate adversarial examples on LFW [32] dataset with the same watermark (only trained on CelebA test set). Besides, we also randomly select 100 facial images from films as additional data to verify the effectiveness of the CMUA-Watermark in more real scenes. It is important to point out that we do not use the additional data to train our adversarial watermark.

The face modification networks we select in our experiments are StarGAN [1], AGGAN [2] and AttGAN [3]. The StarGAN and AGGAN are both trained on CelebA dataset for five attributes: black hair, blond hair, brown hair, gender and aged. These two networks have similar discriminator, and the major difference is that AGGAN introduces attention guided mechanism in generator to improve the quality of fake images compared to StarGAN. Moreover, AttGAN is trained on CelebA dataset for up to fourteen attributes,

which is more complicated compared with the above two networks. As for the test data, [11] randomly selects only 50 facial images in CelebA dataset, but such small test data will cause the results to be contingent. Hence, we evaluate our method on all facial images in CelebA test set and LFW to ensure the credibility.

For every iteration, we run I-FGSM 10 times, and the step size a is 0.01. We find that the hyperparameters in our method have a great influence on our adversarial watermark. Hence, we conduct a lot of experiments with controlled variables to further explore the effect of hyperparameters on the results.

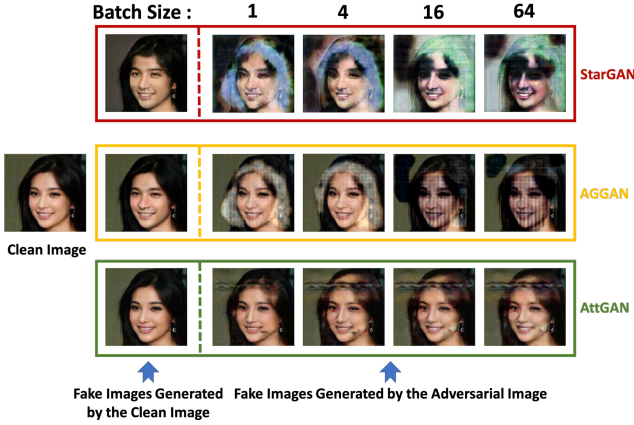


Figure 6. Example results of CMUA-Watermark with different batch sizes. As the batch size increases, the quality of fake images gradually deteriorates.

4.2. Evaluation Metrics

To judge whether the facial image is protected by universal adversarial watermark successfully is not easy, and we design a more reasonable and comprehensive evaluation method for this task after rethinking the purpose of combating deepfake models.

Firstly, one reason we protect facial images is that fake content may show things that someone has not said or done, probably harming the reputation of the person who has been impersonated. To address the issue, the universal adversarial watermark should (1) distort the fake images, (2) lower the quality of fake images and (3) minimize similarity between the $FakeFace_a$ and the $FakeFace_c$. Secondly, considering that many commercial applications are integrated with liveness detection systems which judge whether the input image is from a real person or not, it is very important to protect them from the fake facial images. Hence, we introduce another requirement for the universal adversarial watermark: it should (4) prevent fake faces from passing the verification of liveness detection.

There is no doubt the universal adversarial watermark should be invisible to the human eyes. To ensure that, we use Eq.(2) to control the upper bound magnitude of the watermark.

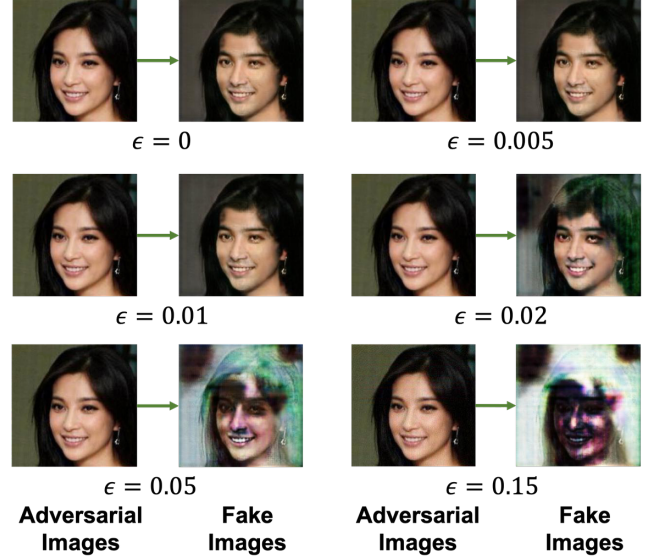


Figure 7. Example results of CMUA-Watermark with different settings of ϵ .

Distortion We use L_2 distance to measure the distortion between the $FakeFace_a$ and $FakeFace_c$. If $L_2 \geq 0.05$, the fake images have noticeable distortions. Hence, [11] suggests that if $L_2 \geq 0.05$ in an image, the perturbation can successfully protect this image. We borrow this idea and calculate the *SuccessRate* [11] for evaluation.

Image Quality The quality of generated images is another key metric worthy of attention. We use FID [12] to measure the quality of fake facial images. FID comprehensively represents the distance of the feature vectors from Inception v3 [33] between two sets of images:

$$FID = \|\mu_o - \mu_f\|_2 + \text{Tr} \left(\Sigma_o + \Sigma_f - 2(\Sigma_o \Sigma_f)^{1/2} \right), \quad (4)$$

where μ_o and μ_f are feature means of original images and fake images respectively, Σ_o and Σ_f are feature covariance matrices of original images and fake images respectively. Obviously, the higher FID indicates the worse quality of the generated images.

Similarity In addition, we use PSNR, SSIM and LPIPS to quantitatively measure the similarity between the $FakeFace_a$ and $FakeFace_c$. Compared to PSNR and SSIM, the results of LPIPS are more consistent with human perception.

Liveness We use an open-source liveness detection system HyperFAS¹ to test the effectiveness of the universal adversarial watermark. The HyperFAS is based on Mobilenet [34] and trained by 360k facial images. In our experiments, if the confidence score of the HyperFAS is greater than 0.95 but less than 0.99, we think the face is a true face with low confidence (TFLC). And if the confidence score is greater than 0.99, we think the face is a true face with high

1. <https://github.com/zeusees/HyperFAS>

confidence (TFHC). Besides, we also calculate the average confidence score ACS for evaluation.

4.3. The Results of Cross-Image Universal Adversarial Watermark

In this section, we discuss the effectiveness and generalization of CIUA-Watermark and report the results in Table 1. Due to the similarity of human faces, the CIUA-Watermark generated by the batch-based universal attack method has ideal performance when the source model is the target model (White-box Attack). Even compared to the SIA-Watermark in [11], the Success Rate [11] of combating StarGAN has not dropped. However, the generalization of CIUA-Watermark is not satisfactory, especially for the case StarGAN- \rightarrow AttGAN. Meanwhile, the metrics of similarity, image quality and liveness detection also perform poorly when the source model is not the target model. Surprisingly, even when the original model is the target model, some metrics of CIUA-Watermark are still inferior to CMUA-Watermark (e.g., the ACS, TFHC and TFLC of AGGAN and AttGAN).

4.4. The Results of Cross-Model Universal Adversarial Watermark

We further investigate the effectiveness of CMUA-Watermark on CelebA test set and LFW in both qualitative and quantitative ways. All experiments in this section use a same configuration of hyperparameters.: decay factor $m = 0.96$, batch size $bs = 64$, upper bound magnitude $\epsilon = 0.05$, and base attack algorithm is I-FGSM. Besides, the adversarial watermark is only trained on CelebA test set.

Figure 1 and Figure 4 show some example results on CelebA and LFW dataset respectively. We can see that, whether the facial image belongs to the dataset used for training or not, the proposed CMUA-Watermark can successfully distort the output images of the deepfake models. Quantitative results of CelebA and LFW are reported in Table 2. Overall, CMUA-Watermark has similar performance on CelebA and LFW, and performs better on StarGAN and AGGAN than AttGAN. Specifically, the *SuccessRate* [11] to combat StarGAN and AGGAN is close to 100% on both CelebA and LFW, which achieves the same performance with [11] without individual training for every image. Besides, the similarity between $FakeFace_a$ and $FakeFace_c$ is poor and the generative quality of $FakeFace_a$ is also bad, which demonstrates that the three models can not modify facial images with the watermark correctly. Moreover, the ACS of $FakeFace_a$ decreases significantly compared with $FakeFace_c$, which makes the TFHC of StarGAN, AGGAN and AttGAN drop 57%, 43.58% and 16.78% respectively on CelebA test set and 40.87%, 36.75% and 6.87% respectively on LFW. The above qualitative and quantitative results both demonstrate that the proposed CMUA-Watermark can successfully protect facial images from multiple deepfake models.

4.5. The Influence of Hyperparameters

The proposed cross-model universal attack pipeline has several hyperparameters which are crucial for the performance. Hence, we systemically investigate how to set them properly.

Decay Factor m

Decay factor m determines the update rate of the universal watermark per iteration, and Figure 5 shows the curves of L_2 , *SuccessRate* [11], *PSNR* and *FID* with it. We can see that: the L_2 scores of StarGAN and AGGAN increase as the decay factor m becomes larger, but the *SuccessRate* [11] of StarGAN and AGGAN no longer increases when m exceeds 0.96. Based on these observations, we suggest setting Decay Factor m as 0.96.

Batch Size bs

The proposed cross-model universal attack pipeline is a batch-based method, and we further explore how to set the batch size bs . As reported in Table 3 and Figure 6, when the bs increases, the performance of the proposed CMUA-Watermark becomes more stable and better, but the gain becomes smaller. Hence, we suggest setting Batch Size bs as 64.

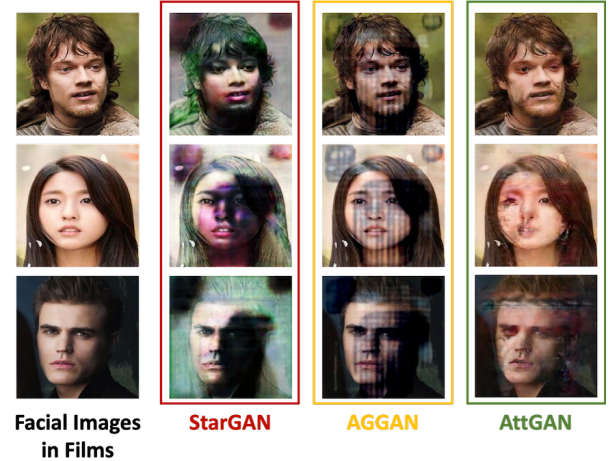


Figure 8. Example results on facial images in films.

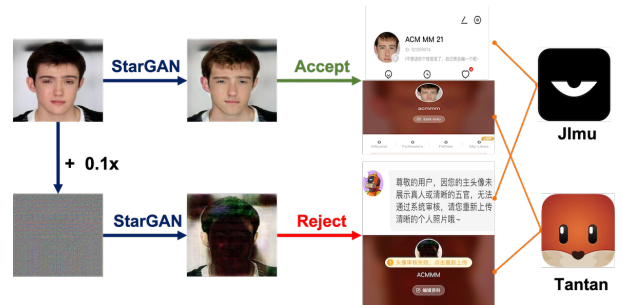


Figure 9. Illustration of using the proposed CMUA-Watermark to prevent fake facial images passing the verification of liveness detection modules integrated by commercial applications.

TABLE 3. THE QUANTITATIVE RESULTS OF CMUA-WATERMARK WITH DIFFERENT BATCH SIZES ON CELEBA TEST SET

<i>bs</i>	Model	L2↑	Success Rate [11]↑	PSNR↓	SSIM↓	LPIPS↑	FID↑	ACS↓	TFHC↓	TFLC↓
1	StarGAN	0.279	99.99%	11.804	0.216	0.421	92.542	0.914->0.530	66.26%->12.59%	80.42%->25.74%
	AGGAN	0.184	100%	13.883	0.463	0.267	31.515	0.928->0.895	65.88%->54.18%	81.46%->74.92%
	AttGAN	0.018	7.30%	25.341	0.707	0.151	19.597	0.872->0.748	55.13%->42.18%	71.20%->58.04%
4	StarGAN	0.325	99.99%	11.184	0.190	0.437	105.872	0.914->0.494	66.26%->11.48%	80.42%->25.02%
	AGGAN	0.188	100%	13.814	0.479	0.257	28.312	0.928->0.861	65.88%->44.65%	81.46%->66.95%
	AttGAN	0.031	17.24%	22.567	0.630	0.217	33.459	0.872->0.719	55.13%->36.02%	71.20%->52.96%
16	StarGAN	0.494	100%	9.270	0.109	0.461	108.526	0.914->0.436	66.26%->11.78%	80.42%->25.10%
	AGGAN	0.127	99.91%	15.585	0.462	0.297	77.381	0.928->0.687	65.88%->25.42%	81.46%->47.92%
	AttGAN	0.036	19.73%	22.010	0.603	0.238	37.513	0.872->0.731	55.13%->37.58%	71.20%->54.70%
64	StarGAN	0.457	100%	9.651	0.121	0.459	115.312	0.914->0.345	66.26%->9.26%	80.42%->19.78%
	AGGAN	0.107	99.21%	16.227	0.476	0.298	87.169	0.928->0.670	65.88%->22.30%	81.46%->43.72%
	AttGAN	0.037	20.20%	21.894	0.599	0.242	38.472	0.872->0.738	55.13%->38.35%	71.20%->55.50%

TABLE 4. THE COMPARISON OF BASE ATTACK ALGORITHMS ON CELEBA TEST SET

Base Method	Model	L2↑	Success Rate [11]↑	PSNR↓	SSIM↓	LPIPS↑	FID↑	ACS↓	TFHC↓	TFLC↓
I-FGSM	StarGAN	0.457	100%	9.651	0.121	0.459	115.312	0.914->0.345	66.26%->9.26%	80.42%->19.78%
	PGD	StarGAN	0.461	100%	9.601	0.124	0.457	111.942	0.914->0.373	66.26%->11.62%
I-FGSM	AGGAN	0.107	99.21%	16.227	0.476	0.298	87.169	0.928->0.670	65.88%->22.30%	81.46%->43.72%
	PGD	AGGAN	0.111	99.65%	16.083	0.464	0.299	85.180	0.928->0.739	65.88%->24.64%
I-FGSM	AttGAN	0.037	20.20%	21.894	0.599	0.242	38.472	0.872->0.738	55.13%->38.35%	71.20%->55.50%
	PGD	AttGAN	0.037	20.22%	21.888	0.598	0.241	38.410	0.872->0.653	55.13%->38.47%

The Upper Bound Magnitude ϵ

As illustrated in Figure 7, the generated fake facial images get more distorted when the parameter ϵ becomes larger, that is, the protection performance becomes better. However, when ϵ becomes too large, the produced adversarial watermark is more likely to be seen. We empirically find that setting ϵ around 0.05 can make a good trade-off between the protection performance and the imperceptibility of the produced adversarial watermark.

Base Attack Algorithm

Our method is built upon the base attack methods, thus we additionally conduct comparison between two widely used base attack methods, i.e., I-FGSM [29] and PGD [30]. The major difference of these two base attack methods is: I-FGSM uses all-zero initial perturbation while PGD uses random noise. In other words, the results of PGD may vary at different executions. In the Table 4, we report the best results achieved by PGD among 5 executions. We can observe that, I-FGSM achieves comparable results with the best ones produced by PGD. Considering that I-FGSM is more stable, we suggest exploiting it as the base attack algorithm of our cross model attack pipeline.

4.6. The Results in Real Scenes

We further evaluate the effectiveness of our CMUA-Watermark in more real scenes.

Facial images in Films. We collect 100 facial images from 10 films to test the effectiveness of the proposed CMUA-Watermark. Though the watermark has not been trained by these facial images ever, our CMUA-Watermark still has an excellent performance on these data as Figure 8 shows. The *SuccessRate* [11] of StarGAN, AGGAN and AttGAN on the protected film images are 100%, 100% and

30.79% respectively, which is even better than it on Celeba test set.

Commercial Applications. One of our goals is to prevent fake facial images passing the verification of liveness detection modules integrated by commercial applications. For example, Some social media platforms require users to upload their real facial images (e.g., Tantan² and Jimu³). As illustrated in Figure 9, we find that some fake images generated by StarGAN can pass the verification of liveness detection of Tantan and Jimu successfully. However, the fake images generated from facial images protected by our CMUA-Watermark can not pass the verification, which demonstrates that our CMUA-Watermark is very effective even in real applications.

5. Conclusion and Future Work

In this paper, we propose a cross-model universal attack pipeline to produce the watermark that can protect thousands of facial images from multiple deep fake models without individual training for every image. Specifically, to alleviate the conflict of adversarial watermarks generated by different facial images, we use the averaged watermark of a batch to update the CMUA-Watermark per iteration. Moreover, according to the purposes of combating deepfake models, we design a more reasonable and comprehensive evaluation method. Experimental results demonstrate that our CMUA-Watermark can effectively protect facial images and prevent the fake facial images passing the verification of liveness detection system. Despite the good generalization ability of our CMUA-Watermark, its performance on the complex models like AttGAN is still not satisfactory. Besides, we

2. <https://apps.apple.com/cn/app/id861891048>

3. <https://apps.apple.com/cn/app/id1094615747>

will try to enhance the generalization of CMUA-Watermark on more deepfake models.

References

- [1] Y. Choi, M. Choi, M. Kim, J.-W. Ha, S. Kim, and J. Choo, "Stargan: Unified generative adversarial networks for multi-domain image-to-image translation," in *Proceedings of the IEEE Conference on Computer Vision and Pattern Recognition*, 2018.
- [2] H. Tang, D. Xu, N. Sebe, and Y. Yan, "Attention-guided generative adversarial networks for unsupervised image-to-image translation," in *International Joint Conference on Neural Networks (IJCNN)*, 2019.
- [3] Z. He, W. Zuo, M. Kan, S. Shan, and X. Chen, "Attgan: Facial attribute editing by only changing what you want," *IEEE Transactions on Image Processing*, vol. 28, no. 11, pp. 5464–5478, Nov 2019.
- [4] A. Rössler, D. Cozzolino, L. Verdoliva, C. Riess, J. Thies, and M. Niessner, "Faceforensics++: Learning to detect manipulated facial images," in *2019 IEEE/CVF International Conference on Computer Vision (ICCV)*, 2019, pp. 1–11.
- [5] N. Bonettini, E. D. Cannas, S. Mandelli, L. Bondi, P. Bestagini, and S. Tubaro, "Video face manipulation detection through ensemble of CNNs," in *International Conference on Pattern Recognition (ICPR)*, 2020.
- [6] S. Tariq, S. Lee, and S. S. Woo, "One detector to rule them all: Towards a general deepfake attack detection framework," in *Proceedings of The Web Conference 2021*, 2021. [Online]. Available: <https://doi.org/10.1145/3442381.3449809>
- [7] D. Afchar, V. Nozick, J. Yamagishi, and I. Echizen, "Mesonet: a compact facial video forgery detection network," in *2018 IEEE International Workshop on Information Forensics and Security (WIFS)*, 2018, pp. 1–7.
- [8] H. Zhao, W. Zhou, D. Chen, T. Wei, W. Zhang, and N. Yu, "Multi-attentional deepfake detection," 2021.
- [9] T. Mittal, U. Bhattacharya, R. Chandra, A. Bera, and D. Manocha, "Emotions don't lie: An audio-visual deepfake detection method using affective cues," in *Proceedings of the 28th ACM International Conference on Multimedia*, ser. MM '20. New York, NY, USA: Association for Computing Machinery, 2020, p. 2823–2832. [Online]. Available: <https://doi.org/10.1145/3394171.3413570>
- [10] K. Chugh, P. Gupta, A. Dhall, and R. Subramanian, "Not made for each other- audio-visual dissonance-based deepfake detection and localization," in *Proceedings of the 28th ACM International Conference on Multimedia*, ser. MM '20. New York, NY, USA: Association for Computing Machinery, 2020, p. 439–447. [Online]. Available: <https://doi.org/10.1145/3394171.3413700>
- [11] N. Ruiz, S. A. Bargal, and S. Sclaroff, "Disrupting deepfakes: Adversarial attacks against conditional image translation networks and facial manipulation systems," in *European Conference on Computer Vision*. Springer, 2020, pp. 236–251.
- [12] M. Heusel, H. Ramsauer, T. Unterthiner, B. Nessler, and S. Hochreiter, "Gans trained by a two time-scale update rule converge to a local nash equilibrium," in *Proceedings of the 31st International Conference on Neural Information Processing Systems*, ser. NIPS'17. Red Hook, NY, USA: Curran Associates Inc., 2017, p. 6629–6640.
- [13] Z. Wang, A. C. Bovik, H. R. Sheikh, and E. P. Simoncelli, "Image quality assessment: from error visibility to structural similarity," *IEEE transactions on image processing*, vol. 13, no. 4, pp. 600–612, 2004.
- [14] R. Zhang, P. Isola, A. A. Efros, E. Shechtman, and O. Wang, "The unreasonable effectiveness of deep features as a perceptual metric," in *CVPR*, 2018.
- [15] M. Li, W. Zuo, and D. Zhang, "Deep identity-aware transfer of facial attributes," *arXiv preprint arXiv:1610.05586*, 2016.
- [16] G. Perarnau, J. van de Weijer, B. Raducanu, and J. M. Álvarez, "Invertible Conditional GANs for image editing," in *NIPS Workshop on Adversarial Training*, 2016.
- [17] J.-Y. Zhu, T. Park, P. Isola, and A. A. Efros, "Unpaired image-to-image translation using cycle-consistent adversarial networks," in *Computer Vision (ICCV), 2017 IEEE International Conference on*, 2017.
- [18] L. Wang, W. Cho, and K.-J. Yoon, "Deceiving image-to-image translation networks for autonomous driving with adversarial perturbations," *IEEE Robotics and Automation Letters*, vol. PP, pp. 1–1, 01 2020.
- [19] C.-Y. Yeh, H.-W. Chen, S.-L. Tsai, and S.-D. Wang, "Disrupting image-translation-based deepfake algorithms with adversarial attacks," 03 2020, pp. 53–62.
- [20] J. Kos, I. Fischer, and D. Song, "Adversarial examples for generative models," in *2018 IEEE security and privacy workshops (spw)*. IEEE, 2018, pp. 36–42.
- [21] P. Tabacof, J. Tavares, and E. Valle, "Adversarial images for variational autoencoders," *arXiv preprint arXiv:1612.00155*, 2016.
- [22] D. Bashkirova, B. Usman, and K. Saenko, "Adversarial self-defense for cycle-consistent gans," in *Advances in Neural Information Processing Systems*, H. Wallach, H. Larochelle, A. Beygelzimer, F. d'Alché-Buc, E. Fox, and R. Garnett, Eds., vol. 32. Curran Associates, Inc., 2019. [Online]. Available: <https://proceedings.neurips.cc/paper/2019/file/b83aac23b9528732c23cc7352950e880-Paper.pdf>
- [23] T.-C. Wang, M.-Y. Liu, J.-Y. Zhu, A. Tao, J. Kautz, and B. Catanzaro, "High-resolution image synthesis and semantic manipulation with conditional gans," in *Proceedings of the IEEE Conference on Computer Vision and Pattern Recognition*, 2018.
- [24] S. Moosavi-Dezfooli, A. Fawzi, O. Fawzi, and P. Frossard, "Universal adversarial perturbations," in *2017 IEEE Conference on Computer Vision and Pattern Recognition (CVPR)*, 2017, pp. 86–94.
- [25] J. H. Metzen, M. C. Kumar, T. Brox, and V. Fischer, "Universal adversarial perturbations against semantic image segmentation," in *2017 IEEE International Conference on Computer Vision (ICCV)*, 2017, pp. 2774–2783.
- [26] J. Li, R. Ji, H. Liu, X. Hong, Y. Gao, and Q. Tian, "Universal perturbation attack against image retrieval," in *2019 IEEE/CVF International Conference on Computer Vision (ICCV)*, 2019, pp. 4898–4907.
- [27] J. Hayes and G. Danezis, "Learning universal adversarial perturbations with generative models," in *2018 IEEE Security and Privacy Workshops (SPW)*. IEEE, 2018, pp. 43–49.
- [28] K. R. Mopuri, A. Ganeshan, and R. V. Babu, "Generalizable data-free objective for crafting universal adversarial perturbations," 2018.
- [29] A. Kurakin, I. J. Goodfellow, and S. Bengio, "Adversarial examples in the physical world," in *5th International Conference on Learning Representations, ICLR 2017, Toulon, France, April 24-26, 2017, Workshop Track Proceedings*. OpenReview.net, 2017.
- [30] A. Madry, A. Makelov, L. Schmidt, D. Tsipras, and A. Vladu, "Towards deep learning models resistant to adversarial attacks," in *International Conference on Learning Representations*, 2018. [Online]. Available: <https://openreview.net/forum?id=rJzIBfZAb>
- [31] Z. Liu, P. Luo, X. Wang, and X. Tang, "Deep learning face attributes in the wild," in *Proceedings of International Conference on Computer Vision (ICCV)*, December 2015.
- [32] G. B. Huang, M. Ramesh, T. Berg, and E. Learned-Miller, "Labeled faces in the wild: A database for studying face recognition in unconstrained environments," University of Massachusetts, Amherst, Tech. Rep. 07-49, October 2007.
- [33] C. Szegedy, V. Vanhoucke, S. Ioffe, J. Shlens, and Z. Wojna, "Re-thinking the inception architecture for computer vision," 06 2016.
- [34] A. G. Howard, M. Zhu, B. Chen, D. Kalenichenko, W. Wang, T. Weyand, M. Andreetto, and H. Adam, "Mobilenets: Efficient convolutional neural networks for mobile vision applications," 2017.